

Evaluation of SiC Power Diodes against Terrestrial Neutron-Induced Failure at Ground Level

Hiroaki Asai^{*1}, Kenji Sugimoto¹, Isamu Nashiyama¹, Kensuke Shiba¹,
Mieko Matsuda¹, Tadaaki Morimura¹

1 High-Reliability Engineering & Components Corporation (HIREC), Japan

*Email: asai@hirec.co.jp

Keyword(s): Silicon Carbide (SiC), Terrestrial Neutron, Single-Event Burnout (SEB),
RCNP, LANSCE/WNR

Abstract

Terrestrial neutrons cause single-event effects (SEEs) in semiconductor devices, which crucially affect the reliability of electronic systems used in the terrestrial environment. This paper presents evaluation results of high energy neutron-induced single-event burnout (SEB) in silicon carbide (SiC) power diodes and differences between SiC and silicon (Si) devices from the SEB standpoint.

1. Introduction

High energy neutrons, protons, pions and muons are produced in nuclear cascade showers created by nuclear reactions between cosmic rays and atmospheric nuclei. Charged particles are halted in a relatively short range, but neutrons produce a cascade of nuclear reactions (air shower) that eventually make terrestrial neutrons at the ground level. High energy neutron-induced single event effects (SEEs) in semiconductor devices, such as Power MOSFET, IGBT, silicon carbide (SiC) devices, SRAM and DRAM, crucially affect the reliability of electronic systems in the terrestrial environment [1-8]. Among them, single-event burnout (SEB) is one of the most serious problems causing fatal damage to electric systems. The SEB is initiated by energetic secondary ionizing atoms induced by neutrons within the semiconductor devices. In the high electric field region of a reversely-biased power device, the initial charge deposited by the secondary atoms is amplified through avalanche multiplication. As a consequence, power devices are short-circuited and broken down to be permanently damaged. In IGBTs and MOSFETs, the ion-induced massive carrier multiplication may result in the turn-on of parasitic bipolar transistors, which will also lead to permanent device failure [9-11].

SiC has been said to have far more suitable characteristics for high voltage and high temperature power device applications than silicon (Si), and SiC power devices are now in the phase of practical applications. However, their reliability against the terrestrial neutrons is not known yet and almost no information on SEB in SiC power devices is available at present.

We have been investigating neutron-induced SEB in high voltage power devices such as SiC diodes, Si diodes and IGBTs. To ensure world-wide consistency of the experimental data presented in this study, we have developed a transportable proton recoil detector (TPRD) to measure high flux and high energy neutron used for SEE testing, and measured neutron fluences at LANSCE/WNR (Los Alamos Neutron Science Center / Weapons Neutron Research) in the USA as well as RCNP (Research Center for Nuclear and Physics) in Japan [12].

This paper demonstrates that differences of device manufacturers and device structures have a strong influence on terrestrial neutron SEB susceptibility. We performed neutron-induced SEB testing in SiC and Si power diodes by using the spallation neutron beam at RCNP. The neutron SEB tolerance of SiC diodes is different by a manufacturer even though they have the same voltage ratings. Also, we discuss similarity between neutron-induced SEB and proton-induced SEB.

2. Experimental

The spallation neutron beam course has been recently developed at RCNP to simulate terrestrial neutrons for neutron-induced SEE testing [13]. Fig. 1 shows the neutron energy spectrum measured at RCNP by Japan Atomic Energy Agency (JAEA) research group in cooperation with RCNP and HIREC along with the spallation neutron spectrum of the WNR, the terrestrial neutron spectrum at sea level [14]. The RCNP neutron spectrum simulated by the Particle and Heavy Ion Transport code System [15] (PHITS) is also shown in Fig. 1. The spectrum of the RCNP spallation neutrons reproduces well the terrestrial neutron spectrum multiplied by 1.5×10^8 in the energy range from 5 MeV to 300 MeV [16].

We used commercially available SiC Schottky diodes as test samples for neutron-induced SEB testing. To evaluate the variation in SEB tolerance, we applied two different SiC diodes with the same voltage rating (600 V) from different manufacturers (A and B) and Si diodes for the purpose of reference. SiC diode B and Si diode B are from the same manufacturer.

The neutron-induced SEB testing circuit in accordance with the MIL standard (MIL-STD-750E Method 1080: Single event burnout and single event gate rupture test) is shown in Fig. 2. Ten test samples of the Devices

Under Test (DUT) are connected in parallel on a DUT board and are reversely biased during neutron irradiation. When one of test samples is subjected to SEB by neutron irradiation, the fuse of the burnout sample blows out to disconnect the sample from the power line. Therefore, neutron-induced SEB testing is continuously performed until all test samples are burned out by neutron irradiation or until the preset time when the SEB testing is terminated, which is called type I (time-truncated) censoring [17]. Irradiation neutron flux was kept constant during the test. The reverse current of test samples is consistently monitored by a measurement system during neutron irradiation. SEB occurrence is judged when the reverse current increases abruptly to cause destructive permanent damage of test samples. Fig. 3 shows schematic experimental configuration. All the neutron irradiation was performed at normal incidence with almost uniform neutron beam. The test samples on the DUT board were placed in the neutron beam, and measurement systems and the high voltage power supply (HVPS) were remotely controlled by a personal computer (PC) in the measurement room. This measurement system detects an abrupt increase in reverse current of the test sample caused by SEB.

3. Experimental Results

Experimental results obtained at RCNP are shown in Fig. 4, which shows the dependence of the SEB cross section on applied voltage. The vertical axis indicates SEB cross section (reciprocal of the fluence at which SEB occurs), and the horizontal axis indicates applied voltage. SEB occurred by neutron irradiation at 600 V, 650 V and 700 V in all test samples. At 500 V and 550 V, SEB occurred only in SiC diode A (Manufacturer A).

Though the experimental data scatter widely by more than an order of magnitude, we could say that the SEB cross sections of SiC diode A (Manufacturer A) are about ten times higher than those of SiC diode B (Manufacturer B), indicating manufacturer difference affects strongly on neutron SEB tolerance of SiC diodes.

When the test results of SiC diode B (Manufacturer B) and Si diode B (Manufacturer B) are compared at 600 V (rating voltage), the SEB cross section difference is not clear because the SEB cross sections of Si diodes scatter in a very wide range of more than three orders of magnitude. This scattering is partly caused by the randomness of the neutron strike location in the diode, and also suggests that sample DUTs should be carefully selected to keep data consistency in the neutron SEB testing.

Fig. 5 shows the number of surviving devices normalized to the sample size as a function of fluence for SiC diode A. So, Fig. 5 indicates an experimental reliability function. The plots decrease monotonically and gradient increases with applied voltage. The plots are fitted by exponential curves. These curves reproduce the major part of the experimental data fairly well, indicating constant failure rate. It is worth of remark that initial failure and wear-out failure are suggested at higher bias voltages in Fig. 5.

The size of the burnout trace is about from 0.05 mm to 0.2 mm in diameter. The location of the burnout trace of the SiC diode and Si diode differs chip by chip spreading over the diode surface [13].

4. Discussion

Neutron burnout phenomena are considered to be random failure (Bernoulli trial) and have a constant failure rate. We performed neutron SEB testing by type I (time-truncated) censoring. In this case, the Maximum Likelihood Estimate (MLE) of failure rate, λ , at an applied voltage can be calculated by,

$$\lambda = \frac{r}{\sum_{i=1}^r t_i + (n-r)T}, \quad (1)$$

where, t_i , T , r , and n are exact time when i 'th failure occurs, censored time, total number of SEB occurrence, and sample size, respectively [17].

Fig. 6 shows the comparison between the present experimental results and those of reference [9], where the vertical axis is in estimated failure in time (FIT). The estimated FIT are calculated by,

$$FIT = \lambda \times \frac{\Phi_{terr}}{\Phi_n} \times 10^9, \quad (2)$$

where, Φ_{terr} and Φ_n are the terrestrial neutron flux and the spallation neutron flux applied in SEB testing. The experimental data of SiC diode A in Fig. 6 show very weak dependence on an applied voltage (electric field). This suggests that crystalline defects in a SiC wafer have an influence on terrestrial neutron SEB susceptibility. Estimated FIT of the SiC diode A and SiC diode in reference [9] show fairly good agreement except at 600 V. Our experimental data of Si diode B link continuously to the Si diode in reference [9] in spite of the difference in the manufacturer. In reference [9], the SiC diode shows higher FIT than the Si diode up to the rated voltage (600 V), indicating the SiC diode is more vulnerable than the Si diode to neutron-induced SEB. Whereas, in our experiment, difference in FIT between the SiC diode A and the Si diode B is not clear at the rated voltage (600 V). It should be noted that the estimated FIT of SiC diode A is significantly higher than that of SiC diode B.

The mechanism of neutron-induced SEB is believed to be similar to that of proton-induced SEB as well as neutron-induced and proton-induced single-event upsets (SEUs) have similar upset mechanism [18]. In order to confirm this, we compare the present data of neutron-induced SEB with those of proton-induced SEB obtained

by Kuboyama *et al.* [10] for SiC power diodes from the same manufacture. Therefore, we applied the same method of analysis as used by Kuboyama *et al.* [10], [13]. Fig. 7 shows the median rank plots (symbols) where $F_i(i, n)$ is plotted against the fluence when i 'th failure occurs and fitting curves of the cumulative failure distribution function (lines) for SiC diode A. Fig. 7 also shows data plots and fitting curves from reference [10] for mono-energetic 70 MeV protons irradiation. As shown in Fig. 7, the entire test data are successfully fitted by the curves and a trend of the results agree with that of reference [10]. Therefore, similar to the proton-induced SEB, neutron SEB is caused by a single high energy neutron without cumulative effect, and triggered by the secondary particles generated by the nuclear reaction between terrestrial neutrons and the substrates of SiC and Si devices. It will be reasonable to assume that the neutrons produce the secondary particles that, in turn, trigger the SEBs. On the contrary to the 70 MeV proton irradiation results in reference [10], the median rank curve is not much affected by the bias voltage in the case of neutron irradiation. The reason is not clear yet, but may be related with the fact that neutrons have broad energy spectrum up to 392 MeV as shown in Fig. 1.

To evaluate the secondary particles generated by the nuclear reaction between terrestrial neutrons and the substrates of SiC and Si devices, we calculated about secondary particles by using PHITS simulation [13]. Through these PHITS simulation results, major difference between SiC device and Si device is secondary carbon atoms. Amount of the secondary carbon atoms in SiC device is much larger than that in Si device, and these energetic carbon atoms may increase SEB cross section, because they have higher energy and longer flight length than secondary energetic silicon atoms [13]. We will examine how these PHITS results have an influence on the mechanism analysis of the SEB occurrence in the future.

5. Summary

We performed testing of high energy neutron-induced SEB in SiC and Si power diodes by using the spallation neutron beam at RCNP. The neutron SEB tolerance of SiC diodes is different by a manufacturer by an order of magnitude even though they have the same voltage ratings. Some SiC diodes are burned out at very low voltages, showing no significant dependence on an applied voltage and that SEB threshold voltage may be strongly affected by crystalline defects in a SiC wafer. By comparing the neutron-induced SEB to the proton-induced SEB by using median rank method, the neutron SEB is triggered by the secondary particles generated by the nuclear reaction between terrestrial neutrons and the substrate of SiC. The PHITS Monte Carlo simulation indicates that secondarily generated energetic carbon nuclei may play important role in the SEB triggering mechanism in SiC power devices. We will examine how crystalline defects have an influence on the internal electric field and the mechanism of neutron-induced SEB in the future.

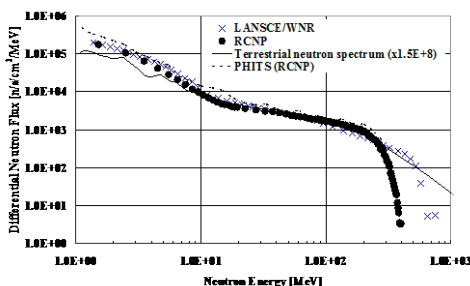


Fig. 1 Comparison of RCNP neutron energy spectrum with LANSCE/WNR neutron spectrum, the PHITS simulation spectrum for RCNP, and terrestrial neutron spectrum at sea level multiplied by 1.5×10^8 [13].

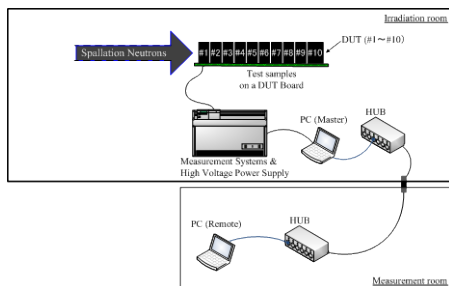


Fig. 3 Schematic experimental configuration of neutron-induced SEB testing. The test samples on the DUT board were placed at the center of the neutron beam, and the measurement systems and the HVPS were remotely controlled by a PC in the measurement room.

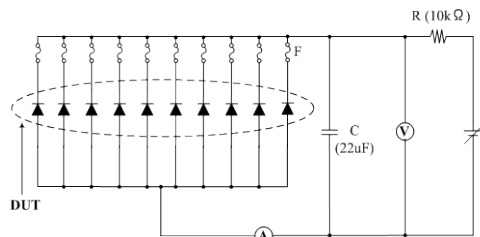


Fig. 2 Circuit diagram of neutron-induced SEB testing. Ten test samples of DUT are connected in parallel and are reversely biased during neutron irradiation.

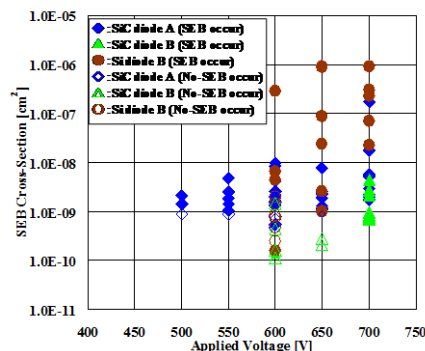


Fig. 4 Applied voltage dependent SEB cross-section of SiC diode A, SiC diode B, and Si diode B. The filled symbols are for SEB occurrence, and the open symbols are for no-SEB occurrence up to the fluence at which tests are terminated.

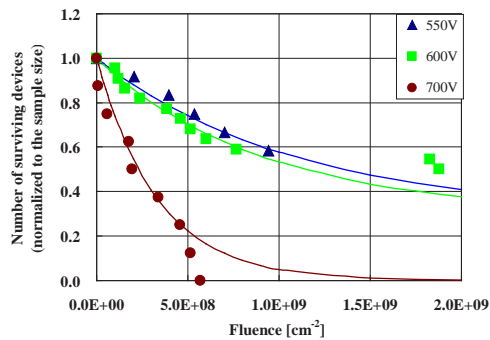


Fig. 5 Number of surviving devices versus neutron fluence for SiC diode A. The number of surviving devices is normalized to the sample size. Solid lines are exponential fitting curves to the experimental data plots.

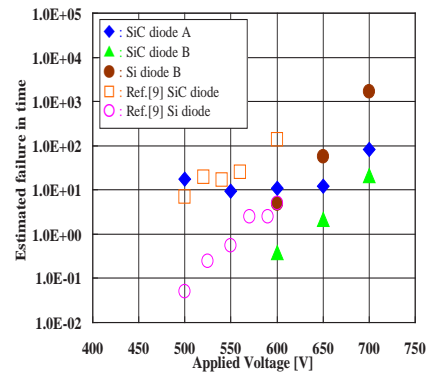


Fig. 6 Estimated failure in time (FIT) versus Applied Voltage. The experimental FIT and that of the reference [9] were compared.

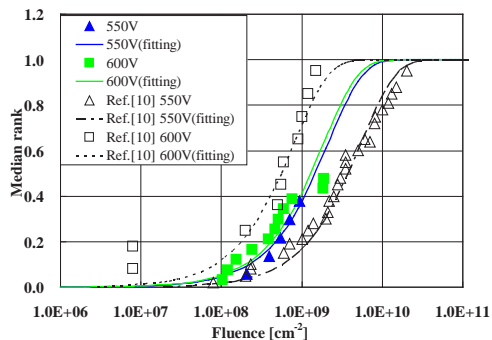


Fig. 7 Median rank plots (symbols) as a function of fluence and fitting curves of cumulative failure distribution functions (lines) for SiC diode A (neutron irradiation) and reference [10] (proton irradiation).

References

- [1] H.R. Zeller, *Microelectron. Reliab.*, vol. 37, No. 10/11, pp. 1711-1718, 1997.
- [2] E. Normand et al., *IEEE Trans. Nucl. Sci.*, vol. 44, pp. 2358-2366, 1997.
- [3] D.L. Oberg et al., *IEEE Trans. Nucl. Sci.*, vol. 43, pp. 2913-2920, 1996.
- [4] Ch. Findeisen et al., International Foundation HFSJG, Activity Report, 1999/2000.
- [5] Th. Stiasny, International Foundation HFSJG, Activity Report, 2005.
- [6] S. Nishida et al., in proceedings of the 22th International Symposium on Power Semiconductor Devices & ICs, 2010.
- [7] E. Normand, *IEEE Trans. Nucl. Sci.*, vol. 43, pp. 2742-2750, 1996.
- [8] H. Kobayashi, *IEEE Proc. IRPS Symp.*, pp. 288-293, 2004.
- [9] G. Soelkner, *Materials Science Forum*, vol. 556-557, pp. 851-856, 2007.
- [10] S. Kuboyama et al., *IEEE Trans. Nucl. Sci.*, vol. 54, pp. 2379-2383, 2007.
- [11] L. Scheick, *IEEE Radiation Effects Data Workshop*, pp. 58-62, 2007.
- [12] H. Asai et al., in proceedings of the 8th European Workshop on Radiation Effects on Components and Systems, 2008.
- [13] H. Asai et al., *IEEE Trans. Nucl. Sci.*, vol. 59, pp. 880-885, 2012.
- [14] Y. Iwamoto et al., *Nuclear Technology*, vol. 173, pp. 210-217, 2011.
- [15] H. Iwase et al., *J. Nucl. Sci. Technol.*, 39, pp. 1142-1151, 2002
- [16] K. Sugimoto et al., in proceedings of the 9th International Workshop on Radiation Effects on Semiconductor Devices for Space Applications, 2010
- [17] NIST/SEMATEC e-Handbook of Statistical Methods, <http://www.itl.nist.gov/div898/handbook/>, June 2010.
- [18] JEDEC Standard JESD89A, Oct. 2006